Self-interaction-corrected density-functional formalism. I. Ground-state properties of the Hubbard-Peierls model

J. A. Majewski and P. Vogl
Physik Department and Walter Schottky Institut, Technische Universität München, D-8046 Garching, Germany
(Received 26 May 1992)

We present detailed studies of the self-interaction-corrected local-spin-density method. As an application, we consider ground-state properties of a highly correlated many-electron system interacting with phonons, namely, the one- and two-dimensional Hubbard-Peierls model. An efficient minimization method is presented which allows one to find fully self-consistent solutions to the self-interaction-corrected local-spin-density total-energy functional without assuming any symmetry of the one-electron states. Charge- and spin-correlation functions, the energy gap, and phonon-induced electronic energy gains for the two-dimensional Hubbard-Peierls model are in significantly better agreement with numerically exact results than the standard local-density method. Noticeably, we find that phonons tend to destabilize the antiferromagnetic ground state in two dimensions and show a negative-U behavior in the energy gap, in contrast to the situation in one dimension. This is relevant for the theory of high-temperature superconductivity.

I. INTRODUCTION

The density-functional theory of Hohenberg, Kohn, and Sham[1] provides an exact mapping of the ground-state properties of a system of many interacting electrons onto a system of noninteracting particles. In practice, however, the exact exchange-correlation part of the total-energy functional is unknown and replaced by an approximate functional. Virtually all modern electronic structure calculations in solids and many in atoms and molecules are based on the local-density approximation (LDA) or local-spin-density (LSD) approximation. The LDA and LSD have an impressive history of successes in describing a wide variety of electronic properties of atoms, molecules, and solids.[2]

On the other hand, a number of deficiencies of the LDA and LSD have also become apparent in recent years.[2] In the case of free atoms, the local-density approach predicts negative ions such as H^-, O^-, and F^- to be unstable and yields too diffuse electron densities. Moreover, the LDA systematically overestimates ionization energies, whereas the calculated *s-p* and *s-d* transfer energies are somewhat too small.

In solids, the LDA (LSD) severely underestimates the band gaps in semiconductors and insulators by typically 50% or more. Also, the predicted cohesive energies of condensed systems lie above the experimental values.[2] Generally, the discrepancy between theory and experiment is larger for properties of surfaces and finite systems than for bulk properties. The LDA also underestimates the stability of antiferromagnetic phases which became particularly apparent in the predictions of the insulating phase of high-temperature superconductors such as La_2CuO_4 and $YBa_2Cu_3O_6$ (for a review, see Ref. 3). In addition, the LDA also fails to predict the antiferromagnetic ground state of several transition-metal oxides.[2]

Presently there is an intense search for systematic improvements of electronic structure calculations.[2] One possibility to go beyond the LDA (LSD) was pointed out several years ago by Perdew and Zunger.[4] In the exact density functional for a single electron system, the Hartree electrostatic energy should be exactly cancelled by the exchange-correlation term. Owing to the approximate character of LDA or LSD, however, this is not the case within these schemes. Consequently, there remains a spurious unphysical self-interaction of the electron with itself. One consequence is the effective one-electron potential in the Kohn-Sham equations[1,2] to possess an incorrect asymptotic behavior at large distances. Perdew and Zunger proposed to subtract the self-interaction energy of all occupied one-electron states from the LDA (LSD) total-energy functional for a many-electron system. This defines the self-interaction-corrected local-density (SIC-LDA) or local-spin-density (SIC-LSD) approximation.

Since the self-interaction correction to the effective one-electron potential depends on the individual electron states, the total electron potential becomes orbital dependent. As a consequence of this orbital dependence, the SIC Hamiltonian is no longer invariant under a unitary transformation among the occupied orbitals—unlike the LDA (LSD) Hamiltonian. These orbitals must be determined self-consistently in such a way that the SIC ground-state energy becomes minimal. However, this condition is difficult to implement in real systems. Therefore, much of the work so far has relied on approximate orbitals of some plausible form, e.g., atomic orbitals or some type of Wannier or bond orbitals. In this simplified form, the SIC method has been applied to atoms,[5] molecules,[6,7] insulators,[8–11] semiconductors,[12] *f*-band metals,[13] impurities in isolators,[14] and to the homogeneous electron gas.[15]

Recently, fully self-consistent SIC-LSD calculations for model systems[16–19] and for transition-metal oxides have been reported.[20] It turns out that the self-consistent SIC method yields antiferromagnetic moments and energy

gaps in much better agreement with experiment than the LSD method. Indeed, studies of the one-dimensional Hubbard model have shown[21–23] that the moments, gaps, and total energies predicted by the SIC-LSD method compare very well with the known exact results, in contrast to the LDA or LSD. Since the implementation of the fully self-consistent SIC method for solids is highly nontrivial, further studies of exactly soluble models and critical evaluations of the SIC-LSD method are called for in order to assess the strengths and weaknesses of this approach.

In the present paper we present a detailed study of the self-interaction-corrected density-functional method for the one- and two-dimensional Hubbard-Peierls[21,24] model, which incorporates both electron-electron and electron-phonon interactions. This work generalizes and extends earlier SIC-LSD studies on the simple Hubbard model. The focus is put on the two-dimensional Hubbard-Peierls model which is of substantial interest in the context of high-T_c superconductivity.[25,26] Since the LSD method fails completely to describe highly correlated systems, the Hubbard-Peierls model provides an interesting and stringent test for the capability of the SIC-LSD method to account for the subtle interplay between electron-electron and electron-phonon effects in correlated electron systems.

The present paper is organized as follows. In Sec. II, the self-interaction-corrected local-density formalism is discussed and an efficient method to calculate the ground-state properties is presented. In the following paper, we extend this method to calculate excitation energies in correlated systems. In Sec. III, we apply this formalism to the Hubbard-Peierls model and study several ground-state properties such as total energies, energy gaps (which are defined as ground-state energy differences), and spin- and density-correlation functions. The implications of our results are discussed in Sec. IV.

II. SELF-INTERACTION-CORRECTED LOCAL-DENSITY FORMALISM

A. SIC total-energy functional

In the local-spin-density (LSD) approximation to the density-functional theory, the total-energy functional is a sum of the kinetic energy, external potential, electronic Coulomb and exchange-correlation interaction:

$$E_{\rm tot}=T_0+V_{\rm ext}+U_c+E_{\rm xc}^{\rm LDS} . \tag{2.1}$$

For a molecule or a periodic solid, the term $V_{\rm ext}$ arises from the electron-nucleus—or, in a pseudopotential approach—the electron-ion interaction. We can write these terms in the form

$$V_{\rm ext}[\rho]=\int \rho(\mathbf{r})v_{\rm ion}(\mathbf{r})d\mathbf{r} , \tag{2.2}$$

$$U_C[\rho]=\tfrac{1}{2}\int \frac{\rho(\mathbf{r})\rho(\mathbf{r}')}{|\mathbf{r}-\mathbf{r}'|}d\mathbf{r}\,d\mathbf{r}'=\tfrac{1}{2}\int v_C(\mathbf{r})\rho(\mathbf{r})d\mathbf{r} , \tag{2.3}$$

$$E_{\rm xc}^{\rm LSD}[\rho_\uparrow,\rho_\downarrow]=\int \rho(\mathbf{r})\varepsilon_{\rm xc}(\rho_\uparrow,\rho_\downarrow)d\mathbf{r} . \tag{2.4}$$

Here, $\varepsilon_{\rm xc}(\rho_\uparrow,\rho_\downarrow)$ is the exchange-correlation energy per electron in an electron gas of uniform spin densities $\rho_\uparrow,\rho_\downarrow$. To obtain the density-functional self-consistent-field equations for the one-electron states $\psi_{\nu\sigma}(\mathbf{r})$, one sets equal to zero the variation of $E_{\rm tot}$ with respect to the $\psi_{\nu\sigma}$ under the constraint $\int d\mathbf{r}\,\rho(\mathbf{r})=\int[\rho_\uparrow(\mathbf{r})+\rho_\downarrow(\mathbf{r})]=N$, fixing the total number of electrons. This procedure yields the Kohn-Sham equations, which read (in atomic units)

$$H_{0\sigma}\psi_{\nu\sigma}=\varepsilon_{\nu\sigma}\psi_{\nu\sigma}(\mathbf{r}) , \tag{2.5}$$

$$H_{0\sigma}=-\tfrac{1}{2}\Delta+v_{\rm ion}(\mathbf{r})+v_C(\mathbf{r})+\mu_{\rm xc}^{\sigma}(\mathbf{r}) , \tag{2.6}$$

$$\mu_{\rm xc}^{\sigma}(\mathbf{r})=\frac{\delta E_{\rm xc}^{\rm LSD}[\rho_\uparrow,\rho_\downarrow]}{\delta\rho_\sigma} . \tag{2.7}$$

The spin-density $\rho_\sigma(\mathbf{r})$ for spin $\sigma=\uparrow,\downarrow$ arises from the occupied solutions of these equations,

$$\rho_\sigma(\mathbf{r})=\sum_{\nu}^{\rm occ}|\psi_{\nu\sigma}|^2 . \tag{2.8}$$

We note that occupied one-electron states are labeled by $\nu\sigma$ throughout this paper; the index ν lumps together all quantum numbers apart from the spin σ. For a system consisting of a single electron, the total energy should be equal to the sum of the kinetic energy and the external potential energy, whereas the Coulomb self-energy and the exchange-correlation energy in the functional Eq. (2.1) should exactly cancel each other. This cancellation is incomplete for the approximate exchange-correlation functional in the LSD scheme. In effect, the self-interaction causes each electron to move in a total potential due to all electrons including itself. This self-repulsion raises the filled valence bands with respect to the empty conduction bands and can be viewed as one reason for the underestimation of energy gaps in the conventional LDA or LSD.[2,8–12] The same type of argument also explains the underestimation of antiferromagnetic moments in LSD.

By appending an additional term to the total-energy functional, $U_{\rm SIC}$, one can remove a large part of this residual self-interaction. Following Perdew and Zunger,[4] $U_{\rm SIC}$ is formed as a sum of two distinct contributions in such a way as to remove, as completely as possible, the self-interaction. First, one subtracts from U_C the exact self-Coulomb energy of each occupied orbital, and second, one subtracts from $E_{\rm xc}^{\rm LSD}$ the self-exchange-correlation energy of each occupied orbital. Thus, the self-interaction-corrected (SIC) total-energy functional $E_{\rm tot}^{\rm SIC}$ reads

$$E_{\rm tot}^{\rm SIC}=T_0+V_{\rm ext}+U_C+E_{\rm xc}^{\rm LSD}+U_{\rm SIC} , \tag{2.9}$$

$$U_{\rm SIC}=-\sum_{\nu\sigma}^{\rm occ}(U_C[\rho_{\nu\sigma}]+E_{\rm xc}^{\rm LSD}[\rho_{\nu\sigma},0]) . \tag{2.10}$$

If the LSD exchange-correlation functional were exact, $U_{\rm SIC}$ would vanish identically.[4] This follows from the fact that the Kohn-Sham equations represent equations for noninteracting electrons. Consequently one has

$$U_C[\rho_{\nu\sigma}]+E_{\rm xc}^{\rm exact}[\rho_{\nu\sigma},0]=0 , \tag{2.11}$$

for each individual electron with density $\rho_{\nu\sigma}$. We point out, however, that Eq. (2.11) does not hold for the *total* charge density.

The presence of the individual orbital densities $\rho_{\nu\sigma}(\mathbf{r})$ in the SIC functional implies that—unlike the density-functional Hamiltonian—$U_{\rm SIC}$ is not invariant under a unitary transformation among the occupied orbitals. For extended states, the self-energy correction to the total energy is positive and tends to zero as $N_a^{-1/3}$ as $N_a \to \infty$, since the exchange-correlation part in $U_{\rm SIC}$ is positive and dominates the negative Coulombic part $U_C = O(N_a^{-1})$ for large N_a. For localized Wannier-type states, on the other hand, the SIC correction is obviously of the order of unity [$U_{\rm SIC} = O(1)$]. In this case, the Coulombic SIC contribution dominates and leads to an overall lowering of the total energy. Thus, the SIC functional for the total energy can discriminate between Heitler-London-type localized eigenstates and Bloch-type extended eigenstates and yields a ground state that either consists of a product of Wannier-like states or Bloch states, depending on which solutions give the lower total energy.

Importantly, the explicit orbital dependence of the SIC total-energy functional does not invalidate the variational density-functional basis of the method in its self-consistent form as it is discussed in this paper. Indeed, it was already shown in Ref. 4 that the SIC functional obeys a Hohenberg-Kohn-type theorem in the sense that the SIC total energy [containing an approximate exchange-correlation energy] and the $\rho_{\nu\sigma}(\mathbf{r})$ are functionals of the total density and $E_{\rm tot}^{\rm SIC}$ becomes a minimum for the ground state.

The basic set of equations which need to be solved to determine the ground-state energy in the SIC-LSD scheme in a self-consistent manner follow from a two-step variational minimization procedure.[6,7,10] To specify our notation and make this paper self-contained, we briefly summarize these equations. One wishes to determine self-consistently the set of mutually orthogonal orbitals $\psi_{\nu\sigma}$ giving rise to orbital densities $\rho_{\nu\sigma} = |\psi_{\nu\sigma}(\mathbf{r})|^2$ that minimize the SIC total energy. First, the $E_{\rm tot}^{\rm SIC}$ is required to be stationary with respect to infinitesimal variations of the type

$$\psi_{\nu\sigma} \to \psi_{\nu\sigma} + \alpha \delta\psi \ . \tag{2.12}$$

This leads to the set of equations

$$H_{\nu\sigma}\psi_{\nu\sigma}(\mathbf{r}) = \sum_{\nu'} \lambda_{\nu'\nu}^{\sigma} \psi_{\nu'\sigma}(\mathbf{r}) \ , \tag{2.13}$$

$$\langle \psi_{\nu'\sigma} | \psi_{\nu\sigma} \rangle = \delta_{\nu\nu'} \ , \tag{2.14}$$

$$H_{\nu\sigma} = H_{0\sigma} + V_{\nu\sigma}^{\rm SIC} \ , \tag{2.15}$$

$$V_{\nu\sigma}^{\rm SIC} = \frac{\delta U^{\rm SIC}}{\delta \rho_{\nu\sigma}} = -\left[\int d\mathbf{r}' \frac{\rho_{\nu\sigma}(\mathbf{r}')}{|\mathbf{r}-\mathbf{r}'|} + \mu_{\rm xc}^{\rm LSD}(\rho_{\nu\sigma}, 0) \right] , \tag{2.16}$$

where $H_{0\sigma}$ has been defined in Eq. (2.6), and $V_{\nu\sigma}^{\rm SIC}$ is the SIC potential for a single orbital $\psi_{\nu\sigma}$. As mentioned above, the index $\nu\sigma$ labels all occupied states. If $V_{\nu\sigma}^{\rm SIC}$ were independent of the state ν, one could immediately apply a unitary transformation to Eq. (2.13) and diagonalize the Lagrange parameters λ. In SIC, however, the off-diagonal elements of λ are a key feature in the method and cannot be neglected. The above equation (2.16) has a simple interpretation. The first term on its right-hand side removes the self-Coulomb potential of $|\psi_{\nu\sigma}|^2$ and the second term removes the self-exchange correlation. In most cases, this *SIC potential provides an attractive localizing potential* for each occupied SIC state ($\nu\sigma$) since the (positive) Hartree potential usually exceeds the (negative) exchange-correlation potential, except for very low density. On the other hand, when the self-consistent SIC orbitals turn out to be delocalized Bloch-type states, $V_{\nu\sigma}^{\rm SIC} = O(1/N_a)$ tends to zero and each electron is subject to the same periodic potential as in conventional band theory.

As mentioned above, the SIC total energy is not invariant with respect to all unitary transformations among the occupied states. This leads to the second condition that $E_{\rm tot}^{\rm SIC}$ is stationary not only with respect to Eq. (2.12) but also with respect to rotations among the individual occupied orbitals $\psi_{\nu\sigma}$, i.e., with respect to

$$\psi_{\nu\sigma} \to \psi_{\nu\sigma} + \sum_{\nu'} \alpha_{\nu\nu'} \psi_{\nu'\sigma} \ . \tag{2.17}$$

This leads to the condition that

$$\langle \psi_{\nu'\sigma} | V_{\nu'\sigma}^{\rm SIC} - V_{\nu\sigma}^{\rm SIC} | \psi_{\nu\sigma} \rangle = 0 \tag{2.18}$$

for all pairs ν, ν'. These equations guarantee that the solution of Eqs. (2.13)–(2.16) has the energetically optimal degree of localization and have therefore been termed "localization equations."[6] Since the $\psi_{\nu\sigma}$ are orthogonal to each other, one obtains from Eq. (2.13)

$$\lambda_{\nu'\nu}^{\sigma} = \langle \psi_{\nu\sigma} | H_{\nu'\sigma} | \psi_{\nu'\sigma} \rangle \ . \tag{2.19}$$

Then, Eq. (2.18) reads

$$(\lambda_{\nu\nu'}^{\sigma})^* = \lambda_{\nu'\nu}^{\sigma} \ , \tag{2.20}$$

i.e., the matrix λ must be Hermitian.

Equations (2.13)–(2.16) together with Eq. (2.20) cannot be transformed into an eigenvalue problem and thus appear to be more difficult to solve than the standard LSD equations. However, with the recent advent of efficient direct minimization techniques for electronic structure calculations,[27–30] these equations can actually be solved with comparable effort. An efficient minimization scheme for the SIC-LSD equations is presented in the next section.

B. Minimization procedure

The total energy is a function of the N occupied SIC states $\psi_{\nu\sigma}$. In this section only, we omit the spin index and lump it into the orbital index, such that

$$E_{\rm tot} = E_{\rm tot}(\{\psi_\nu\}) \ . \tag{2.21}$$

In order to find the ground-state energy of the system, one wishes to minimize $E_{\rm tot}$ with respect to the set of ψ_ν, subject to the constraints Eqs. (2.14) and (2.20) for

$\nu,\nu'=1,\ldots,N$. By introducing these conditions via Lagrange multipliers μ and $\tilde{\mu}$, the expression to be minimized becomes

$$\tilde{E}_{\rm tot}=E_{\rm tot}(\{\psi_\nu\})+\sum_{\nu\nu'}\mu_{\nu\nu'}(\langle\psi_\nu|\psi_{\nu'}\rangle-\delta_{\nu\nu'}) +\sum_{\nu\nu'}\tilde{\mu}_{\nu\nu'}(\langle\psi_\nu|V_{\nu'}-V_\nu|\psi_{\nu'}\rangle) . \quad (2.22)$$

At the extremum, the Lagrange multipliers in Eq. (2.22) are shown in the Appendix to be given by

$$\mu_{\nu\nu'}=-\lambda_{\nu\nu'},\quad \tilde{\mu}_{\nu\nu'}=0,\quad \nu,\nu'=1,\ldots,N . \quad (2.23)$$

To accelerate the convergence of the minimization process, it is advantageous not to take these expressions but to choose them in the following form:

$$\mu_{\nu\nu'}=-\tfrac{1}{2}(\lambda^*_{\nu'\nu}+\lambda_{\nu\nu'}) , \quad (2.24)$$

$$\tilde{\mu}_{\nu\nu'}=\lambda^*_{\nu'\nu}-\lambda_{\nu\nu'} , \quad (2.25)$$

with $\lambda_{\nu'\nu}$ given by Eq. (2.19) and ψ taken from the current iteration (see below). The form Eq. (2.24) for μ guarantees that the localization condition is obeyed when the extremum is reached (see the Appendix). The expression for $\tilde{\mu}$ has the important effect to accelerate the convergence into the minimum where λ is Hermitian, since

$$\sum_{\nu\nu'}\tilde{\mu}_{\nu\nu'}\langle\psi_\nu|V_{\nu'}-V_\nu|\psi_{\nu'}\rangle=\sum_{\nu\nu'}(\lambda^*_{\nu'\nu}-\lambda_{\nu\nu'})(\lambda_{\nu'\nu}-\lambda^*_{\nu\nu'}) =\sum_{\nu\nu'}|\lambda_{\nu\nu'}-\lambda^*_{\nu'\nu}|^2 . \quad (2.26)$$

We have used the following variant of the conjugate gradient method in order to efficiently minimize $\tilde{E}_{\rm tot}$. The $(n+1)$th iteration for ψ_ν is obtained from the equation

$$\psi_\nu^{(n+1)}=\psi_\nu^{(n)}+\epsilon^{(n)}h_\nu^{(n)},\quad n=0,1,2,\ldots, \quad (2.27)$$

where $\epsilon^{(n)}$ are small positive constants and $h_\nu^{(n)}$ are generalized gradients given by

$$h_\nu^{(n)}=\sum_{k=0}^{n}\frac{\langle g^{(n)}|g^{(n)}\rangle}{\langle g^{(n-k)}|g^{(n-k)}\rangle}g^{(n-k)} , \quad (2.28)$$

where

$$g^{(n)}\equiv g_\nu^{(n)}=-\delta\tilde{E}(\psi_\nu^{(n)})/\delta\psi_\nu^{(n)} . \quad (2.29)$$

In contrast to the standard conjugate gradient technique, which employs additional line minimizations, we have chosen $\epsilon^{(n)}$ to be a small positive constant independent of n and inversely proportional to a typical energy in the problem. The present method may be considered a blend of the conjugate gradient technique and the steepest-descent method.[28] For the applications presented in Sec. III, we found this scheme to be 5–10 times faster than the steepest-descent method. In principle, line minimizations are more effective than choosing a constant relaxation parameter ϵ. However, it is extremely time consuming to perform line minimizations when subsidiary constraints have to be taken into account.

We have used Eqs. (2.13)–(2.16), (2.22), (2.24), and (2.25) to find the solutions of the SIC equations which minimize the total energy. In general, all ψ_ν need to be varied independently. Often, however, translational and point-group symmetry can be used to reduce the number of independent equations. If all N_a atoms are equivalent, for example, then one has

$$\psi_{\nu'}(\mathbf{r}-\mathbf{R}_{\nu'})=\psi_\nu(\mathbf{r}-\mathbf{R}_\nu) , \quad (2.30)$$

which reduces the number of independent orbitals in the minimization process from N to just 1.

III. THE HUBBARD-PEIERLS MODEL IN THE SELF-INTERACTION-CORRECTED LSD FORMALISM

The discovery of high-temperature superconductivity has revived the theoretical interest in the Hubbard model—particularly in two dimensions—as a simple yet nontrivial model for highly correlated systems.[31] Since this model can be solved (numerically and/or analytically) exactly in limiting cases, it is ideally suited to test the SIC-LSD scheme for a wide range of electronic correlations.

In this section, we investigate a wide range of electronic properties of the one-dimensional (1D) and 2D Hubbard-Peierls model within the SIC-LSD scheme. In particular, we present results for the half-filled Hubbard and Hubbard-Peierls model in the thermodynamic limit (at zero temperature) which is difficult to reach in Monte Carlo simulations.

The Hubbard model for the 1D undistorted lattice can be solved exactly for any band filling.[22,23] However, it is well known that one-dimensional electron systems with a half-filled energy band are unstable against a phonon distortion (Peierls instability) which leads to a dimerized ground state.[24] If the Hubbard Hamiltonian is augmented by an electron-phonon interaction, one obtains the so-called Hubbard-Peierls model. No exact solutions are known for this model; it was studied in 1D within the unrestricted Hartree-Fock method,[32] various variational methods,[33,34] the Monte Carlo method,[35] and—for short chains—by exact numerical diagonalization.[36]

In two dimensions, neither the Hubbard nor the Hubbard-Peierls model is exactly solvable. A variety of approximate techniques has been used to study it, such as the Hartree-Fock method,[37,38] slave-boson mean-field methods,[39,40] Green's-function decoupling schemes,[21,41] functional integral formulations,[42] and variational approaches.[43–45] The most accurate results have been obtained by exact numerical diagonalizations of the Hubbard Hamiltonian[46–49] and by Monte Carlo simulations.[50–56] However, these techniques can only be used for small finite lattices (8–16 sites for exact diagonalizations, and up to 256 sites in Monte Carlo simulations). Whereas the strong quantum fluctuations prevent the formation of long-range spin order and magnetization in 1D, all numerical results so far strongly suggest that the ground state of the half-filled 2D Hubbard model is an antiferromagnetic insulator with opposite spins on neighboring sites for any value of the Coulomb repulsion U.[50] Moreo *et al.*[56] have also studied various ground-state properties for band fillings different from half-filling.

The influence of various phonon distortions on the total energy in the two-dimensional Hubbard-Peierls model was studied for small lattices previously by Monte Carlo as well as exact diagonalization methods.[57–60]

A. The SIC-LSD equations

In this section we develop the SIC-LSD equations for the one- and two-dimensional Hubbard-Peierls model, incorporating both the electron-electron and the electron-phonon interaction. The Hubbard-Peierls model is characterized by the following Hamiltonian:

$$H=\sum_{\langle ij\rangle\sigma} t_0\left[1+\frac{\alpha}{t_0}(\mathbf{u}_i-\mathbf{u}_j)\cdot\mathbf{r}_{ij}\right]\hat{c}^{\dagger}_{i\sigma}\hat{c}_{j\sigma} +\tfrac{1}{2}U\sum_{i\sigma}\hat{n}_{i\sigma}\hat{n}_{i-\sigma} . \tag{3.1}$$

The electron number operators $\hat{n}_{i\sigma}=\hat{c}^{\dagger}_{i\sigma}\hat{c}_{i\sigma}$ are labeled by a site index i and spin σ. We will restrict ourselves to a one-band model with a single s state per site. U is the intra-atomic Coulomb repulsion parameter ($U>0$), t_0 is the nearest-neighbor hopping matrix element for the undistorted lattice, and $\langle ij\rangle$ indicates a sum over nearest neighbors. The lattice is a 1D chain or a 2D square lattice. The undistorted nearest-neighbor distance is denoted by a. A distortion or phonon displacement $\{\mathbf{u}_i\}$ changes t_0 by an amount proportional to the electron-phonon coupling constant α. The vector $\mathbf{r}_{ij}$ is a unit vector pointing from site i to site j.

At zero temperature and for an undistorted lattice, the model Hamiltonian is characterized uniquely by two parameters, that is, the strength of the Coulomb interaction relative to the transfer integral, U/t_0, and the average concentration of electrons N/N_a, where N and N_a are the total number of electrons and lattice points, respectively. The change of the hopping parameter owing to a phonon can be characterized by a dimensionless parameter $\delta=\alpha u_c/t_0$, where u_c is the amplitude of the phonon displacement ($-1\le\delta\le 1$).

For convenience, we measure all energies in units of t_0 and take the orbital energy of the atomic s state as the zero of energy. The wave vectors are given in units of π/a.

In a tight-binding model, the charge density is available only in the form of discrete site occupancies. Consequently, local-density-functional theory cannot literally be applied to such a model. Invoking the spirit of DF theory, however, one may define a discrete version of the LDA, LSD, and SIC-LSD method where Coulomb and exchange-correlation energies are functionals of the local occupancies $n_{i\sigma}\equiv\langle\hat{n}_{i\sigma}\rangle$.[61] This approach has previously been used for the standard Hubbard model.[16,17] Adopting this concept for the present system, we find the following SIC-LSD energy functional for the Hubbard-Peierls model:

$$E_{\rm tot}=T+U[n]+E^{\rm LSD}_{\rm xc}[n,\zeta]+\Delta E^{\rm SIC} , \tag{3.2}$$

$$T=\sum_{\langle ij\rangle\sigma} t_0\left[1+\frac{\alpha}{t_0}(\mathbf{u}_i-\mathbf{u}_j)\cdot\mathbf{r}_{ij}\right]\langle\hat{c}^{\dagger}_{i\sigma}\hat{c}_{j\sigma}\rangle_0 , \tag{3.3}$$

$$U[n]=\tfrac{1}{2}U\sum_i(n_{i\uparrow}+n_{i\downarrow})^2 , \tag{3.4}$$

$$\Delta E^{\rm SIC}=\sum_{\nu}(U[n^{\nu}]+E^{\rm LSD}_{\rm xc}[n^{\nu},1]) , \tag{3.5}$$

where $\langle\hat{c}^{\dagger}_{i\sigma}\hat{c}_{j\sigma}\rangle_0$ is the mean-field average of the operator $\hat{c}^{\dagger}_{i\sigma}\hat{c}_{j\sigma}$. We can write this expectation value more explicitly by expanding the one-electron states $\psi_{\nu\sigma}$ in terms of the tight-binding basis functions $\phi_{i\sigma}$,

$$\phi_{i\sigma}=\hat{c}^{\dagger}_{i\sigma}|0\rangle , \tag{3.6}$$

$$\psi_{\nu\sigma}=\sum_i^{N_a} c_i^{\nu\sigma}\phi_{i\sigma} . \tag{3.7}$$

In terms of this basis, one gets

$$\sum_{\sigma}\langle\hat{c}^{\dagger}_{i\sigma}\hat{c}_{j\sigma}\rangle_0=\sum_{\nu\sigma}^{\rm occ}(c_i^{\nu\sigma})^{*}c_j^{\nu\sigma} . \tag{3.8}$$

In particular, the site occupancy of the state $\nu\sigma$ is given by $n_i^{\nu\sigma}=(c_i^{\nu\sigma})^{*}c_i^{\nu\sigma}$ and the total occupancy of site i with electrons of spin σ is $n_{i\sigma}=\sum_{\nu}^{\rm occ}n_i^{\nu\sigma}$.

Following Ref. 16, we take the LSD exchange-correlation functional in the form

$$E^{\rm LSD}_{\rm xc}[n,\zeta]=U\sum_i n_i^{4/3}\left\{-a-b\frac{(1+\zeta_i)^{4/3}+(1-\zeta_i)^{4/3}-2}{2(2^{1/3}-1)}\right\} . \tag{3.9}$$

The parameters $a=0.3840$ and $b=0.0705$ have been chosen such that the total energy and the position of the spin-down eigenvalue in the atomic limit ($t_{ij}=0$) agree with the conventional LSD results for a free hydrogen atom. The results discussed in this paper, particularly in Sec. III, do not depend critically on these parameters a and b, as will be discussed in Sec. IV. Here, ζ_i and n_i are the spin polarization and the occupancy of site i, respectively,

$$\zeta_i=\frac{n_{i\uparrow}-n_{i\downarrow}}{n_{i\uparrow}+n_{i\downarrow}},\quad n_i=n_{i\uparrow}+n_{i\downarrow} . \tag{3.10}$$

With this exchange-correlation functional, the SIC correction to the total energy, Eq. (3.5), reads

$$\Delta E^{\rm SIC}=-U\sum_{\nu}^{\rm occ}\sum_i^{N}[\tfrac{1}{2}(n_i^{\nu})^2-(a+b)(n_i^{\nu})^{4/3}] . \tag{3.11}$$

Note that the LSD functional for the total energy is given by Eq. (3.2) with the SIC correction set equal to zero. The LDA functional for the exchange-correlation energy, on the other hand, is obtained from the expression Eq. (3.9) with the parameter $b=0$.

The functional derivative of the $E^{\rm SIC}_{\rm tot}$ with respect to the orbital density gives the potential on site i for an electron in the state $\nu\sigma$,

$$V_i^{\nu\sigma}=Un_i+V^{{\rm LSD},\sigma}_{{\rm xc},i}+V_i^{{\rm SIC},\nu\sigma} , \tag{3.12}$$

where $V^{{\rm LSD},\sigma}_{{\rm xc},i}$ is the LSD exchange-correlation potential

and reads for spin up (+) and spin down (−) electrons, respectively,

$$V_{\mathrm{xc},i}^{\mathrm{LSD},(\pm)} = U\tfrac{4}{3} n_i^{1/3} \left\{ -a - \frac{b}{2^{1/3}-1} [(1\pm\zeta_i)^{1/3} - 1] \right\} . \tag{3.13}$$

$V_i^{\mathrm{SIC},\nu\sigma}$ in Eq. (3.12) is the self-interaction correction to the potential $V_i^{\nu\sigma}$, and is given by

$$V_i^{\mathrm{SIC},\nu\sigma} = -U[n_i^{\nu\sigma} - \tfrac{4}{3}(a+b)(n_i^{\nu\sigma})^{1/3}] . \tag{3.14}$$

This is the only potential contribution which depends on the individual electron state $\nu\sigma$.

Employing the method detailed in Sec. II, we can now find the ground-state energy of the Hubbard-Peierls Hamiltonian for any number N_a of atoms, distortion pattern, and number N of electrons. The total-energy functional is minimized with respect to the coefficients $c_i^{\nu\sigma}$, starting with some initial guess. The simplest initial condition is to assume completely localized electron states, $c_i^{\nu\sigma} = \delta(x_{\nu\sigma}, x_i)$. During the minimization process, the coefficients $c_i^{\nu\sigma}$ relax towards the self-consistent solution. This initial condition is very efficient provided the self-consistent SIC orbitals are localized Heitler-London-type solutions.

For a half-filled band, we have used initial conditions with zero total z component of the spin and many different spin orderings in order to ensure the convergence of the SIC-LSD equations to the lowest-energy state. As will be further discussed in Sec. IV, the ground state of both the LSD and the SIC-LSD Hamiltonian for half-filling turns out to be either paramagnetic or antiferromagnetic in any dimension. Thus, the effects of quantum fluctuations for large U, particularly in 1D systems—which cannot possess a symmetry broken ground state[62]—are still not fully captured by the SIC-LSD method. However, the qualitative as well as quantitative improvements brought about by this scheme compared to the standard LSD or LDA will be seen to be considerable. In the remainder of this section we focus on the antiferromagnetic state.

B. Results for the 2D Hubbard-Peierls model on a 4×2 lattice

First, we present results for various correlation functions for a small finite Hubbard-Peierls system, namely a square lattice consisting of two rows of four atoms each. For such a small system, one can compare the SIC-LSD solutions with the results from an exact numerical diagonalization of the Hamiltonian Eq. (3.1) and assess the accuracy of the self-interaction-corrected density-functional scheme.

Employing iterative diagonalization techniques,[63] we have first calculated the exact eigenstates of the Hamiltonian Eq. (3.1) on a 4×2 square lattice for a half-filled band [i.e., constant site occupancy $n_i = 1$]. For an 8-site lattice, there are 16 available one-electron states. Since these states are occupied by 8 electrons, this gives $\binom{16}{8} = 12\,870$ many-body basis states. Since states with different total z component of the spin, S_z, do not couple with one another, it suffices to diagonalize much smaller submatrices. The Hamiltonian matrix corresponding to $S_z = 0$, for example, leads to a 4900×4900 matrix. Only this matrix is needed to compute the ground state.[48,64]

The small size of the lattice causes additional degeneracies of the ground state for small U, which can be lifted by suitable boundary conditions. There are only two possibilities on a 4×2 lattice, namely either periodic or antiperiodic conditions along the x direction (i.e., the direction with four atoms) and periodic ones along the y direction. Doubly antiperiodic boundary conditions are equivalent to periodic ones for this lattice. In order to obtain results on the 4×2 lattice which agree with the results on an infinite lattice for $U = 0$, we employed periodic boundary conditions for all total-energy differences (Secs. III B 1, III B 2, and III B 4) but antiperiodic ones for all correlation functions (Sec. III B 3). For large U, the two types of boundary conditions give identical results.

1. *Influence of phonons on the ground-state energy*

The total electronic energy of the Hamiltonian Eq. (3.1) can be lowered by zone-boundary phonons.[57,60] In this section, we consider those two types of distortion patterns $\mathbf{u}_i = \mathbf{u}_0 \cos(\mathbf{q}\cdot\mathbf{r}_i)$ which give the largest gain in the electronic energy. These are the longitudinal acoustic (LA) zone-boundary phonons (i) with phonon wave vector $\mathbf{q}^{(1)} = (\pi/a, 0)$, and (ii) with wave vector $\mathbf{q}^{(2)} = (\pi/a, \pi/a)$, where a denotes the undistorted nearest-neighbor distance.

In Fig. 1, we present the SIC-LSD and LSD results and compare them to the exact ground-state energy for the undistorted lattice—as obtained from the diagonalization of Eq. (3.1). The SIC method slightly overestimates the ground-state energy for small U but yields a considerable overall improvement on the standard local-spin-density method.

In Fig. 2, the same type of comparison is shown for the electronic energy gain $E_{\mathrm{tot}}(U,0) - E_{\mathrm{tot}}(U,\delta)$ due to the $(\pi/a, 0)$ phonon as a function of U. The phonon amplitude is given by $\delta = \alpha|\mathbf{u}_0| = 0.1$ and the displacement pattern is indicated as an inset in this figure. Figure 3 shows

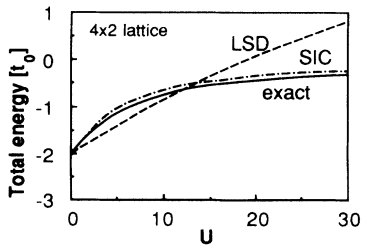

FIG. 1. Comparison of the exact total energy (full line) with the LSD (dashed line) and SIC-LSD (dot-dashed line) approximations for the two-dimensional Hubbard model on a 4×2 square lattice, as a function of the on-site Coulomb repulsion U. The energy in this and all following figures is measured in units of the nearest-neighbor hopping matrix element t_0 which is proportional to the bandwidth.

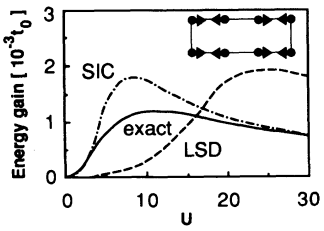

FIG. 2. Electronic energy gain by a lattice distortion in the two-dimensional Hubbard-Peierls model on a 4×2 square lattice as a function of U, calculated by exact diagonalization, LSD, and SIC-LSD, respectively. The frozen-in lattice displacement corresponds to a $(\pi/a,0)$ phonon and is shown in the inset. The relative change in the hopping matrix element δ is 0.1.

the corresponding results for the longitudinal $(\pi/a,\pi/a)$ phonon. As can be deduced from the exact results shown in these figures, the electronic energy gain by the $(\pi/a,\pi/a)$ phonon is smaller than that of the $(\pi/a,0)$ phonon for values of $U<15.7$ but the opposite holds for larger U. This crossing of the energies was the subject of a controversy in Refs. 58 and 59. In the SIC-LSD approximation, the energy gain for the $(\pi/a,0)$ phonon is always lower and approaches the one by the $(\pi/a,\pi/a)$ phonon for $U\rightarrow\infty$.

These figures demonstrate the rather dramatic failure of the standard LSD method to predict the subtle interplay between the electron-electron and electron-phonon interaction in a correlated many-electron system. The SIC-LSD method, on the other hand, corrects most of these errors in the entire regime of U.

2. Energy gap

The energy gap of an insulator can be defined by[65]

$$E_{\rm gap}=[E_{\rm tot}(N+1)-E_{\rm tot}(N)]-[E_{\rm tot}(N)-E_{\rm tot}(N-1)]\ , \tag{3.15}$$

with $E_{\rm tot}(N)$ denoting the ground-state energy for N electrons. In Fig. 4, different calculations of $E_{\rm gap}/U$ as a function of U for the undistorted 4×2 lattice are compared to one another. Note that for $U\rightarrow\infty$, one has $E_{\rm gap}/U\rightarrow 1$. For the half-filled 1D Hubbard model and for a three-band 2D Hubbard model in the context of high T_c materials, similar calculations have been performed in Refs. 16 and 17, respectively. The notorious underestimation of the energy gap by the standard LSD or LDA method is evident from Fig. 4. The SIC-LSD

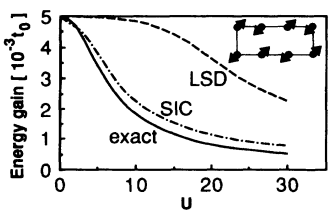

FIG. 3. Analogous to Fig. 2, but for a $(\pi/a,\pi/a)$ phonon, as indicated in the inset.

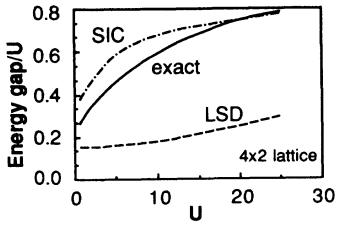

FIG. 4. The energy gap in the half-filled two-dimensional Hubbard model on a 4×2 square lattice, as a function of U and measured in units of U.

method, on the other hand, gives much better agreement with the exact results but tends to somewhat overestimate the energy gap in the intermediate regime of U values.

3. Correlation functions

Spin- and density-correlation functions in a correlated electron system provide a stringent test for approximate models. We have computed several correlation functions in the present mean-field-type schemes, namely LSD and SIC-LSD. In this section, these results are compared to exact ones obtained by diagonalization of the many-body Hamiltonian. In a one-band Hubbard model, a lattice site may be empty, singly, or doubly occupied. We introduce operators for the spin at site i, $S_i^z=\hat{n}_{i\uparrow}-\hat{n}_{i\downarrow}$, the local density $\hat{n}_i=\hat{n}_{i\uparrow}+\hat{n}_{i\downarrow}$, and the double occupancy at site i, $\hat{D}_i=\hat{n}_{i\uparrow}\hat{n}_{i\downarrow}$. In addition, we define cross-correlation functions $C_{ij}^{XY}=\langle X_i Y_j\rangle$, where X and Y represent one of the quantities S^z, $\hat{n}$, or $\hat{D}$, and the brackets indicate the many-electron ground-state expectation value.

The exact ground-state wave function can be written as a linear combination of Slater determinants $|G\rangle$,

$$|\Psi\rangle=\sum_G a_G|G\rangle\ , \tag{3.16}$$

$$|G\rangle=\hat{c}_{i_1\uparrow}^{\dagger}\cdots\hat{c}_{i_{N_\uparrow}\uparrow}^{\dagger}\hat{c}_{j_1\downarrow}^{\dagger}\cdots\hat{c}_{j_{N_\downarrow}\downarrow}^{\dagger}|0\rangle\ . \tag{3.17}$$

The operators $c_{i\uparrow}^{\dagger}$ and $\hat{c}_{i\downarrow}^{\dagger}$ create electrons in the basis specified in Eq. (3.6), and $i_{k\uparrow}$ $(1\le k\le N_\uparrow)$ and $j_{l\downarrow}$ $(1\le l\le N_\downarrow)$ label the sites occupied by the $N_\uparrow$ electrons with spin up, and $N_\downarrow$ electrons with spin down, respectively. The summation in Eq. (3.16) extends over all possible configurations $|G\rangle$ with a given total $S_z=N_\uparrow-N_\downarrow$ (note that S_z commutes with the Hamiltonian). The number of different configurations $|G\rangle$ for given S_z is equal to $\langle{N_a\atop N_\uparrow}\rangle\cdot\langle{N_a\atop N_\downarrow}\rangle$, where N_a is the total number of lattice sites.

In effective mean-field-type theories such as LSD and SIC-LSD, the expansion coefficients in Eq. (3.16) are given by the product of the $(N_\uparrow+N_\downarrow)$ coefficients $c_i^{\nu\sigma}$,

$$a_G^{\text{SIC-LSD}}=c_{i_1}^{1\uparrow}\cdots c_{i_{N_\uparrow}}^{N_\uparrow\uparrow}c_{j_1}^{1\downarrow}\cdots c_{j_{N_\downarrow}}^{N_\downarrow\downarrow}\ . \tag{3.18}$$

Here, the $c_i^{\nu\sigma}$ are defined in Eq. (3.7), and result from the minimization of the total-energy functional in Eq. (3.2). The calculation of the correlation functions within the LSD or SIC-LSD schemes is straightforward but requires

some tedious operator algebra. For this purpose, it is useful to introduce the matrix elements $P_{ij\sigma}$,

$$P_{ij\sigma}=\langle\Psi|\hat{c}^{\dagger}_{i\sigma}\hat{c}_{j\sigma}|\Psi\rangle \ . \tag{3.19}$$

Within mean-field schemes, all correlation functions can be expressed in terms of these matrix elements, $P_{ij\sigma}$. Using Eqs. (3.16)–(3.18), they read

$$P_{ij\sigma}=\sum_{\nu=1}^{N_\sigma}(c_i^{(\nu\sigma)})^{*}c_j^{(\nu\sigma)} \ . \tag{3.20}$$

Another useful relation which facilitates the calculations and is valid for single Slater determinants is[66]

$$\begin{aligned}\langle\Psi|\hat{n}_{i\sigma}\hat{n}_{j\sigma}|\Psi\rangle&=\langle\Psi|\hat{n}_{i\sigma}|\Psi\rangle\langle\Psi|\hat{n}_{j\sigma}|\Psi\rangle-P^2_{ij\sigma}\\&=P_{ii\sigma}P_{jj\sigma}-P^2_{ij\sigma} \ .\end{aligned} \tag{3.21}$$

In the present study, we have calculated the density-density and spin-spin correlation functions, $\rho_{ij}=\langle\hat{n}_i\hat{n}_j\rangle$ and $q_{ij}=\langle S_i^zS_j^z\rangle$, respectively, both for the exact many-body ground state of the Hubbard Hamiltonian as well as within the LSD and SIC-LSD approximations. The Fourier transforms of the correlation functions ρ_{ij} and q_{ij} are the density-density structure factor $S_{\rm den}(\mathbf{q})$ and the magnetic spin-spin structure factor $S_{\rm mag}(\mathbf{q})$,

$$S_{\rm den}(\mathbf{q})=\frac{1}{N_a}\sum_{ij}\exp[i\mathbf{q}(\mathbf{R}_i-\mathbf{R}_j)]\rho_{ij} \ , \tag{3.22}$$

$$S_{\rm mag}(\mathbf{q})=\frac{1}{N_a}\sum_{ij}\exp[i\mathbf{q}\cdot(\mathbf{R}_i-\mathbf{R}_j)]q_{ij} \ . \tag{3.23}$$

The latter function is a measure of the antiferromagnetic long-range order in the system.

In the limit $U=0$, the ground state is paramagnetic and represents a completely delocalized Bloch state. In this limit, the correlation functions have the following values: $\rho_{ii}=\langle n_i^2\rangle=\frac{3}{2}$; $\rho_{ij}=\langle n_in_j\rangle=\frac{1}{2}$ $(i\neq j)$; $q_{ii}=\langle S_{iz}^2\rangle=\frac{1}{2}$; and $q_{ij}=\langle S_{iz}S_{jz}\rangle=-\frac{1}{2}$ $(i\neq j)$. In an antiferromagnetic Néel state, on the other hand, one has $\rho_{ij}=1$ for all i and j, and $q_{ij}=1$ ($q_{ij}=-1$) if i and j lie on the same (opposite) spin sublattice.

We begin our discussion with the double occupancy $D_i=\langle\hat{n}_{i\uparrow}\hat{n}_{i\downarrow}\rangle$, which is depicted in Fig. 5 as a function of U. This figure illustrates the significant overall improvement achieved by the SIC-LSD method on the standard LSD results. An important implication of this result is that the electron-electron interaction energy, given by $U\sum_i D_i$, is much more accurately accounted for in the SIC-LSD method.

We have calculated $S_{\rm mag}(\mathbf{q})$ for various $\mathbf{q}$ vectors and found $S_{\rm mag}(\mathbf{q})$ to be sharply peaked at $\mathbf{q}=(\pi/a,\pi/a)$, both for the exact ground state and for the mean-field approximations (SIC-LSD,LSD). Indeed, the vector $(\pi/a,\pi/a)$ is the nesting vector for the Brillouin zone of a square lattice at half-filling which drives the antiferromagnetic instability.[67] The magnitude of $S_{\rm mag}(\mathbf{q})$ as a function of U turns out to be grossly overestimated by SIC-LSD, however. This is shown in Fig. 6. Both SIC-LSD and LSD theory predict $S_{\rm mag}(\pi/a,\pi/a)$ to reach the perfect Néel state value N_a for $U\rightarrow\infty$ since these approaches do not properly take into account spin fluctuations and always favor the broken symmetry solution with wave vector $(\pi/a,\pi/a)$. In the limit $U\rightarrow\infty$, any spin configuration without double site occupancies is an eigenstate of the Hubbard Hamiltonian and contributes to the many-electron wave function, whereas only the Néel state contributes in a mean-field-type scheme. Slave boson mean-field methods[40] yield similar discrepancies.

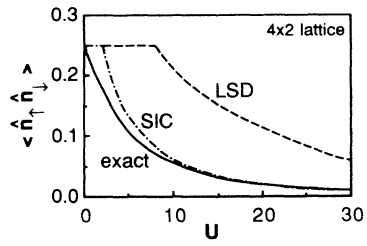

FIG. 5. The mean double occupancy on one atomic site in the two-dimensional half-filled Hubbard model on a 4×2 square lattice, as a function of U, calculated by exact diagonalization, LSD, and SIC-LSD, respectively. For $U<8$ and $U<2.5$, the self-consistent LSD and SIC-LSD solutions are paramagnetic, respectively, and antiferromagnetic for larger U.

When spin fluctuations do not play an essential role, however, the SIC-LSD calculation is in very good agreement with the exact many-body result, in contrast to the standard LSD method. This is illustrated in Fig. 7 for the case of the density-density structure factor $S_{\rm den}(\pi/a,\pi/a)$ and in Fig. 8 for the local spin moment L_0,

$$\begin{aligned}L_0&=\langle S_{iz}^2\rangle\\&=\langle\hat{n}_{i\uparrow}+\hat{n}_{i\downarrow}-2\hat{n}_{i\uparrow}\hat{n}_{i\downarrow}\rangle\\&=\langle\hat{n}_{i\uparrow}\rangle+\langle\hat{n}_{i\downarrow}\rangle-2D_i \ .\end{aligned} \tag{3.24}$$

Note that L_0 involves only D_i. Figure 8 demonstrates the notorious underestimation of the local spin moment by the LSD method which leads to its well-known underestimation of antiferromagnetism.

Figures 6–8 exhibit another difference between the exact and the spin-density results on the 4×2 square lattice. Both SIC and LSD solutions show an artificial "phase transition" from the delocalized paramagnetic to the localized antiferromagnetic solution at some critical $U_{\rm thr}$. Below this threshold, only paramagnetic solutions exist

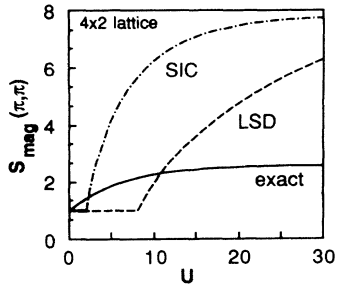

FIG. 6. The spin-spin structure factor $S_{\rm mag}(\pi/a,\pi/a)$ in the two-dimensional half-filled Hubbard model on a 4×2 square lattice.

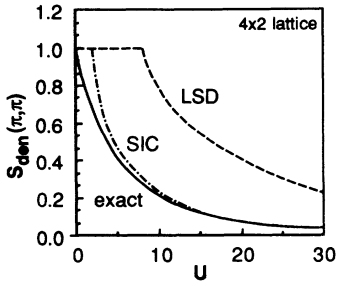

FIG. 7. The density-density structure factor $S_{\rm den}(\pi/a,\pi/a)$ in the two-dimensional half-filled Hubbard model on a 4×2 square lattice.

both for the LSD and SIC-LSD equations. However, the SIC-LSD scheme yields a much smaller threshold value than the LSD method and additionally shows the correct asymptotic limit $U_{\rm thr}\to 0$ for $N_a\to\infty$, in contrast to the LSD method (see Sec. IV A).

4. *Exact density functional*

The present tight-binding representation of density-functional theory allows a direct comparison of the exact exchange-correlation density functional for the 4×2 system with the approximate expressions of the LSD and SIC-LSD schemes. The density functional may generally be defined as[61]

$$E_{\rm DF}=E_{\rm tot}-E_{\rm kin}^{\rm nonint}-E_{\rm Hartree}\ , \tag{3.25}$$

where $E_{\rm kin}^{\rm nonint}$ is the kinetic energy of the noninteracting electrons and $E_{\rm Hartree}$ is the Hartree Coulomb energy. In the present model system, $E_{\rm kin}^{\rm nonint}$ equals the total ground-state energy for $U=0$ which can be evaluated analytically.

The exact, SIC-LSD, LSD, and LDA density functionals in the ground state, as defined by Eq. (3.25), are depicted in Figs. 9 and 10 as a function of U. Figure 9 shows the half-filled band case ($\langle n\rangle=1$), whereas Fig. 10 shows the density functionals for the half-filled band containing one hole ($\langle n\rangle=\frac{7}{8}$). The difference between these two figures shows the effects of doping which are poorly described in the LSD approximation. For the whole range of U, the SIC exchange-correlation functional lies very close to the exact one. This is particularly relevant for the theory of high-T_c materials where the effects of doping play a crucial role.

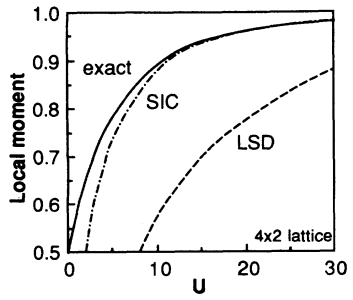

FIG. 8. The local spin moment on one atomic site $\langle S_z^2\rangle$ in the two-dimensional half-filled Hubbard model on a 4×2 square lattice.

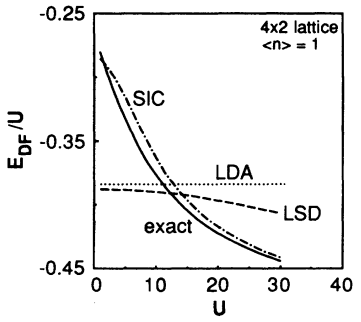

FIG. 9. Comparison of the exact density functional in the half-filled Hubbard model ($\langle n\rangle=1$) on a 4×2 square lattice with the approximate LDA, LSD, and SIC-LSD functionals.

C. SIC-LSD results for the 2D Hubbard-Peierls model on larger lattices

It will be demonstrated in this section that the SIC-LSD method renders possible systematic studies of very large lattices where finite-size effects are negligible.

1. *Total energies and hole binding energies*

As we have seen, the SIC-LSD method captures most properties of highly correlated electrons in the Hubbard model quantitatively, in contrast to the standard LSD or LDA method. The only exception are properties which depend sensitively on quantum fluctuations. This finding remains valid also for larger lattices. In Table I, several correlation functions and electronic energies obtained with the SIC-LSD method are compared with previously obtained exact results[48] on 4×4 lattices. For 8×8 lattices, our SIC-LSD calculations give total electronic energies of -0.871 (-0.86 ± 0.04), -0.536 (-0.53 ± 0.04), and -0.289 (-0.28 ± 0.06) for $U=4$, 8, and 16, respectively, in excellent agreement with recent Monte Carlo results[54] which are cited in parentheses.

Additionally, we compare the binding energy of two holes $\Delta=(E_2-E_0)-2(E_1-E_0)=(E_2-E_1)-(E_1-E_0)$

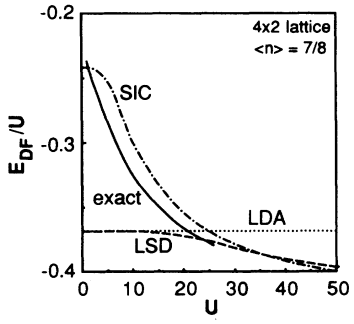

FIG. 10. Comparison of the exact density functional in the Hubbard model on a 4×2 square lattice with the approximate LDA, LSD, and SIC-LSD functionals. The average electron density amounts to $\langle n\rangle=\frac{7}{8}$.

TABLE I. Several electronic ground-state properties calculated by the SIC-LSD method, the LSD method, and by exact diagonalization (Ref. 48), for the two-dimensional Hubbard model on a 4×4 square lattice for $U=4$ and two different band filling factors. The table contains the total energy per atom E_{tot}/N_a, the kinetic energy per atom E_{kin}/N_a, the local spin moment $\langle S_z^2\rangle$, the on-site density fluctuation $\langle n^2\rangle$, and the density-density structure factor $S_{den}(\pi/a,\pi/a)$.

	E_{tot}/N_a	E_{kin}/N_a	$\langle S^2\rangle$	$\langle n^2\rangle$	$S_{den}(\pi/\pi)$
		$\langle n\rangle=1$ (half-filled band)			
Exact	−0.851	−1.312	0.76	1.23	0.39
SIC	−0.857	−1.329	0.67	1.27	0.47
LSD	−1.076	−1.493	0.44	0.59	0.62
		$\langle n\rangle=14/16$ (two holes)			
Exact	−0.984	−1.337	0.70	1.05	0.42
SIC	−0.944	−1.394	0.67	1.13	0.54
LSD	−1.258	−1.488	0.54	1.28	0.62

as obtained by SIC with Monte Carlo simulations for a 4×4 square lattice[68] (cf. Fig. 11). E_n denotes the energy of the ground state with n holes. This quantity is particularly relevant in the context of pairing and the formation of a bosonic condensate. It has been suggested that the ground state of the Hubbard model for small deviations from half-filling is unstable against the formation of domain walls resulting in an incommensurate antiferromagnet.[69] Such a transition does not occur in the SIC-LSD approach. We have used various initial conditions with partially localized holes, but always obtained a ground state with fairly localized holes and a Néel-type magnetic ordering far away from the holes. As a consequence, the SIC-LSD only qualitatively predicts the dependence of Δ as a function of U (see Fig. 11).

2. *Electronic energy gain by lattice distortions*

For larger values of U, the eigenstates of the electronic system in the SIC-LSD method are localized Heitler-London type states and approach an antisymmetric product of atomic wave functions for $U\rightarrow\infty$. Quantities such as the total energy converge very rapidly to their limiting value on infinite lattices. For $U\geq 2$, for example, the total energy in the 112-site (14×8) lattice differs from the one for the 512-site lattice by less than 0.5%.

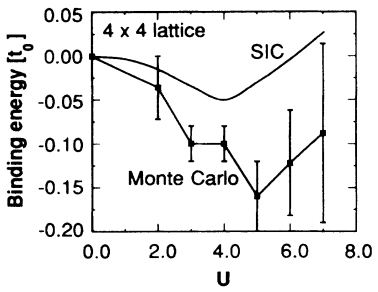

FIG. 11. Comparison of Monte Carlo (from Ref. 68) with the present SIC-LSD results for the binding energy of two holes in the Hubbard model on a 4×4 square lattice.

We have studied in some detail the electronic energy gain associated with four different distortion patterns: (i) two superimposed phonons with eigenvectors $\mathbf{e}(\mathbf{q})=\mathbf{e}(\pi/a,0)\|(1,0)$ and $\mathbf{e}(0,\pi/a)\|(0,1)$; the LA phonons (ii) $\mathbf{e}(\pi/a,0)\|(1,0)$, (iii) $\mathbf{e}(\pi/a,\pi/a)\|(1,1)$, and (iv) $\mathbf{e}(\pi/a,\pi/a)\|(1,0)$. So far, the effect of those distortions on the ground state of Eq. (3.1) was investigated only for $U=0$ or on very small lattices where some of these phonons are degenerate with one another.[57,60]

For the distortion pattern of type (iii), the 2D system dissociates into weakly coupled vibrating chains, while patterns of type (i) lead to weakly coupled breathing 2×2 plaquettes. A complete dissociation is reached for the phonon amplitude $\delta=1$. For both limiting cases, the exact solutions of the Hubbard-Peierls model are known.[57]

In Fig. 12, we depict the energy gain for these phonons on a 32×16 lattice, as predicted by the present SIC-LSD calculations. For phonons of type (i), one finds a very different behavior of the electronic energy gain as a function of U than for the 4×2 lattice (cf. Fig. 2). This difference is primarily caused by the higher symmetry and mode degeneracy on the 4×2 lattice. The electronic energy gain for the other distortion patterns is qualitatively similar to the small lattice case. In particular, the gain for the phonons of type (iii) and (iv) for large U are practically identical to gain for the distortion patterns (i) and (ii), respectively.

3. *Energy gap: 2D versus 1D Hubbard-Peierls system*

A physically unexpected result of this study is shown in Fig. 13. We have calculated the energy gap Eq. (3.15) of the 2D half-filled Hubbard-Peierls system as a function of the distortion (iii). For comparison, in Fig. 14 we also show the energy gap of the 1D chain as a function of dimerization amplitude δ for several values of U. In the latter case, a zone-boundary phonon induces an energy gap which is *enhanced* by the electron-electron interaction U. In other words, both the electron-phonon and the electron-electron interaction tend to stabilize an insulating ground state in one dimension and increase the energy gap. In two dimensions, however, the situation is exactly reversed: the 2D Hubbard-Peierls model exhibits

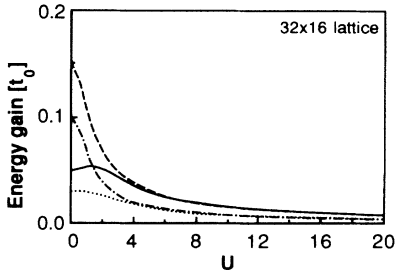

FIG. 12. Electronic energy gain by four different lattice distortion patterns as described in the text [type (i), full line; type (ii), dotted line; type (iii), dashed line; type (iv), dash-dotted line] in the two-dimensional Hubbard-Peierls model on a 32×16 square lattice as a function of U, as predicted by the SIC-LSD method. The relative change in the hopping matrix element is $\delta=0.3$.

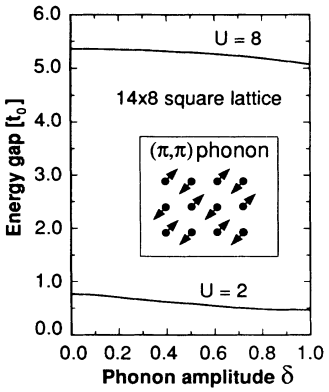

FIG. 13. Calculated energy gap for the half-filled two-dimensional Hubbard model, as predicted by the present SIC-LSD method, as a function of the $(\pi/a,\pi/a)$ phonon displacement δ indicated in the inset and for two values of the Coulomb repulsion U.

a negative-U behavior. Whereas there is a finite energy gap for nonzero U, the phonon distortions always diminish it.

The physical origin of this difference lies in the different effect of a phonon distortion in 1D and in 2D. Irrespective of the dimension, the electron-ion interaction favors double occupancy, whereas the Coulomb repulsion U favors single occupancy of the orbitals (antiferromagnetic state). Thus, a lattice distortion always leads to a higher double occupancy in the short bonds. This bond order diminishes the spin order and corresponds to an effective reduction of U. Consequently one finds that the derivative $\partial E_{\rm gap}/\partial U$ decreases with increasing distortion amplitude both in 1D and in 2D Hubbard-Peierls systems.

In a 1D half-filled Hubbard-Peierls chain, there is an energy gap already for $U=0$ which is proportional to the distortion amplitude δ, as shown in Fig. 14. For $U\to\infty$, on the other hand, δ will have a smaller and smaller influence since the ground state approaches that of completely decoupled atoms. Thus, for $U=\infty$, the energy gap as well as all other observables become independent of δ. For finite values of U, the energy gap lies smoothly in between these limiting cases, as can be seen from Fig. 14. This figure also shows clearly that $\partial E_{\rm gap}/\partial U$ decreases with δ.

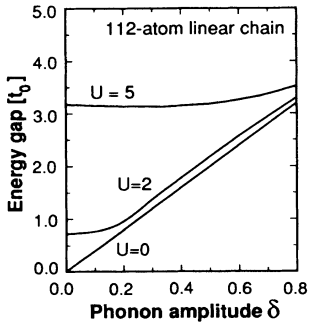

FIG. 14. Calculated energy gap for the half-filled one-dimensional Hubbard model, as predicted by the present SIC-LSD method, as a function of the phonon displacement δ and for various values of the Coulomb repulsion U.

In a 2D system, on the other hand, the phonon distortions alone do not produce a charge gap, i.e., for $U=0$ there is no energy gap. The reason is simply that ionic displacements along any one-dimensional direction cannot open a gap everywhere on the two-dimensional Fermi surface simultaneously. For finite U, the phonon distortions do contribute to a charge gap but the decrease of $\partial E_{\rm gap}/\partial U$ as a function of δ now ensures not only a relative decrease (as in 1D) but also an absolute decrease of the energy gap. *Thus, in two dimensions, phonons destabilize an antiferromagnetic ground state.* For very large U, however, in both 1D and 2D systems the influence of the phonons on the energy gap becomes negligible.

D. Dimerization in the 1D Peierls-Hubbard model

In the infinite 1D Hubbard-Peierls chain, the bond alternation—called Peierls distortion—in the ground state results from a competition between the gain in electronic energy and the loss of elastic energy. Both Monte Carlo results[35] and studies based on the Gutzwiller ansatz[34] have shown that the bond alternation amplitude δ changes nonmonotonically as a function of U (see Fig. 15). In contrast, Hartree Fock studies have not been able to reproduce the initial increase in δ for small U. This phenomenon therefore gives another stringent test for the SIC-LSD method.

First, we augment the Hamiltonian Eq. (3.1) by an elastic energy,

$$H_{\rm elastic}=\tfrac{1}{2}K\sum_n (u_n-u_{n+1})^2\ , \tag{3.26}$$

where u_i is the displacement of the ith atom from its lattice site, and K is the elastic force constant. For $U=0$, this Hamiltonian is the Su-Schrieffer-Heeger[70] (SSH) Hamiltonian which can be solved exactly. The one-electron energy gap in the electronic spectrum is given by $E_{\rm gap}=4\alpha u_c$, where $u_c=|u_i-u_{i+1}|$. The dimerization

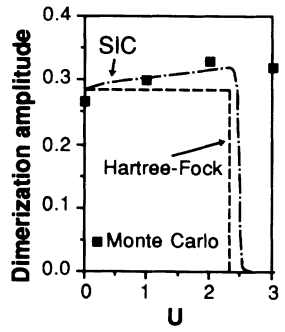

FIG. 15. Calculated equilibrium dimerization amplitude δ_0 vs the on-site repulsion U for a half-filled 24-atom chain. The dimensionless elastic energy constant is $\lambda=0.29$. The dashed line indicates unrestricted Hartree-Fock results of Ref. 35, the dash-dotted line shows the present SIC-LSD results, and the squares are the results of Ref. 35 from quantum Monte Carlo simulations.

amplitude $\delta=\alpha u_c$ equals the relative change in the hopping matrix element with the lattice distortion u_c. In addition, the elastic energy is determined by the parameter $\lambda=2\alpha^2/(\pi K)$. The amplitude δ_0 in the dimerized ground state follows from the minimization of the energy

$$E_0=NKu_c^2+E_{\text{tot,el}} , \tag{3.27}$$

where $E_{\text{tot,el}}$ is the total electronic energy. In Fig. 15, we show the dimerization δ_0 versus U for a 24-atom chain, as obtained by Monte Carlo, unrestricted Hartree-Fock[35] (UHF) and the present SIC-LSD method. The elastic energy parameter λ was chosen to be $\lambda=0.29$. We note that the SIC-LSD results are already converged with respect to the lattice size.

Both the UHF and the standard LSD method (without SIC correction) predict a dimerization δ_0 which is *independent* of U up to a threshold value of U, and zero beyond. For UHF, this threshold value is $U=2.32$ (Fig. 15), whereas it is $U=9.45$ for plane LSD.

The present SIC results correctly mimic the exact results for small U and predict the initial increase of δ quantitatively. The small difference in δ for $U=0$ stems from the different treatment of the phonons in this work and in Ref. 35. For larger U, however, the SIC-LSD approach predicts the dimerization to vanish at $U=2.5$, where a finite antiferromagnetic spin-polarization develops.

The exact ground state of the Hamiltonian Eq. (3.1) has zero spin polarization ζ_i. In LSD as well as SIC-LSD, on the other hand, the ground state is antiferromagnetic and develops a finite polarization ζ_i, which is related to the local moment by

$$\langle S_{iz}^2\rangle=\tfrac{1}{2}(1+\zeta_i^2) . \tag{3.28}$$

The exact ground state does possess a local moment, but the quantum fluctuations in 1D suppress the formation of a magnetization for any U. This is the origin of the slow decrease of the dimerization for larger U. Since these fluctuations are not accounted for accurately in the SIC-LSD method, this method also fails to reproduce the dimerization in the limit of large U.

IV. DISCUSSION OF THE SIC METHOD

A. Driving mechanisms for the antiferromagnetism in SIC-LSD and LSD

Both in the LSD and the SIC-LSD method, the ground state of the Hubbard Hamiltonian in 1D and 2D is antiferromagnetic for sufficiently large U. In spite of this similarity, the single-electron solutions of the LSD and SIC-LSD Hamiltonians are radically different from each other. In the LSD approach, the electron potential for a given spin polarization is periodic, which leads to eigenstates in the form of extended Bloch states. In contrast, the SIC potential for electron $\nu\sigma$ is attractive on site x_ν; correspondingly, the one-electron solutions of the SIC-LSD equations can be localized states corresponding to a Mott insulator. In the atomic limit ($U\to\infty$) the ground state in the SIC-LSD method is a product of isolated neutral atoms, whereas in the LSD method the electron eigenstates are Bloch states with different amplitudes on both spin sublattices.

In this section we show that the physical mechanisms which produce an antiferromagnetic (AF) ground state differ considerably in the conventional LSD theory and in the present SIC-LSD method. We will demonstrate this explicitly for the Hubbard model, but we believe the conclusions of this section to be more generally valid. Basically, in LSD the driving mechanism for an AF ground state is the exchange-correlation energy [see Eq. (3.9)], whereas it is the Hartree contribution to the self-interaction correction, $\sum U[n^\nu]$ in Eq. (3.5), in the SIC-LSD method.

In order to understand this difference, it is illuminating to consider the limiting case of an H_2 molecule in the present tight-binding scheme. In this case, there are four basis states which we label by $(i\sigma)$. Here, $i=1,2$ denote the atoms and $\sigma=\uparrow,\downarrow$ the spin. The Hamiltonian reads

$$H=t_0(\hat{c}_{1\uparrow}^\dagger\hat{c}_{2\uparrow}+\hat{c}_{2\uparrow}^\dagger\hat{c}_{1\uparrow}+\hat{c}_{1\downarrow}^\dagger\hat{c}_{2\downarrow}+\hat{c}_{2\downarrow}^\dagger\hat{c}_{1\downarrow}) +U(\hat{n}_{1\uparrow}\hat{n}_{1\downarrow}+\hat{n}_{2\uparrow}\hat{n}_{2\downarrow}) . \tag{4.1}$$

We will again measure all energies in units of t_0. There is only one independent occupancy which we choose to be $x\equiv\langle\hat{n}_{1\uparrow}\rangle$. Symmetry and normalization then give $\langle\hat{n}_{2\uparrow}\rangle=1-\langle\hat{n}_{1\uparrow}\rangle, \langle\hat{n}_{2\downarrow}\rangle=\langle\hat{n}_{1\uparrow}\rangle;\quad \langle\hat{n}_{1\downarrow}\rangle=1-\langle\hat{n}_{1\uparrow}\rangle$. In addition to x, it is convenient to define $\epsilon=x-1/2$. Both in the LSD and SIC-LSD method, the site occupancy x is then determined by the equation

$$x=\tfrac{1}{2}[1+z^2g^2(x)+zg(x)\sqrt{1+z^2g^2(x)}]^{-1} , \tag{4.2}$$

where $z=U/2$ and $g(x)$ is given by [see Eqs. (3.13) and (3.14)]

$$g^{\text{LSD}}(\epsilon)=V_{\text{xc},1}^{\text{LSD},\uparrow}-V_{\text{xc},1}^{\text{LSD},\downarrow} =-b\frac{4}{3}\frac{2^{1/3}}{2^{1/3}-1}[(\epsilon+\tfrac{1}{2})^{1/3}-(\tfrac{1}{2}-\epsilon)^{1/3}] , \tag{4.3}$$

$$g^{\text{SIC}}(\epsilon)=V_1^{\text{SIC},1\uparrow}-V_1^{\text{SIC},1\downarrow} =-2\epsilon+\frac{4}{3}\left[a-b\left[\frac{2^{1/3}}{2^{1/3}-1}-1\right]\right] \times[(\epsilon+\tfrac{1}{2})^{1/3}-(\tfrac{1}{2}-\epsilon)^{1/3}] , \tag{4.4}$$

respectively. There is an important difference between these equations. $g^{\text{SIC}}(\epsilon)$ contains a term -2ϵ which originates in the Hartree term of the self-energy correction and is independent of the exchange-correlation parameters a and b. On the other hand, $g^{\text{LSD}}(\epsilon)$ is proportional to the small parameter b.

One set of solutions of Eq. (4.2) is the spin-unpolarized solution $\epsilon=0$ which corresponds to $g^{\text{LSD}}(0)=g^{\text{SIC}}(0)=0$. We can obtain another solution for x or ϵ from Eq. (4.2) by expanding its right-hand side up to second order in ϵ, assuming ϵ is small. This procedure leads to the solution

$$\epsilon\cong\frac{2+zg'(0)}{-\frac{3}{2}z^2(g'(0))^2} , \tag{4.5}$$

where $g'(0)=(dg/d\epsilon)|_{\epsilon=0}$. This equation only gives a

positive solution for ϵ provided

$$zg'(0) < -2 \ . \tag{4.6}$$

From Eqs. (4.3) and (4.4) we see that $(dg^{\mathrm{SIC}}/d\epsilon)|_{\epsilon=0}$ contains a constant term (-2) which is independent of the parameters of the exchange-correlation functional. For the parameters a,b given in Sec. III A, one obtains $g'(0) = -2+0.16 = -1.84$ for SIC-LSD and $g'(0) = -0.4833$ for LSD implying a spin-polarized solution to exist for $U/2 > 2.17$ and $U/2 > 8.28$ in the SIC-LSD and the LSD method, respectively.

It is now evident that the early onset of antiferromagnetism (AF) in SIC-LSD, which can also be seen in Figs. 5–8, is caused by the Hartree self-energy. These threshold values for U agree well with the numerical solutions of Eq. (4.2). This analysis also explains why the SIC-LDA functional [i.e., Eq. (3.9) with $b=0$] gives results very similar to the SIC-LSD functional.

As noted already in Sec. III B 3, the threshold values for U, U_{thr} depend on the system's size. By considering increasingly larger lattices, we have found that U_{thr} tends to zero within numerical accuracy, in excellent agreement with the exact many-body results.

The general conclusion of this section is that the transition to the AF ground state in the SIC-LSD method does not depend sensitively on the local exchange-correlation functional, in contrast to the LSD approach.

B. Paramagnetic solutions of the SIC Hamiltonian — comparison of the SIC-LSD and LDA method

So far, we have focused on the antiferromagnetic solution of the Hubbard Hamiltonian in 1D and 2D, which forms the ground state for sufficiently large U in the SIC-LSD method. In principle, this method should yield the lowest energy solution automatically which may be antiferromagnetic (AF) or paramagnetic (PM), depending on the strength of the Coulomb interaction. Unfortunately, however, the PM solution of the SIC-LSD Hamiltonian is much more difficult to obtain than the AF solution for an extended system because of its extremely slow convergence towards a bulk limit.

As a concrete example, we consider the Hubbard Hamiltonian in the SIC-LSD approximation at half-filling for a *finite* linear chain with N_a sites. There is a delocalized paramagnetic solution with one-electron eigenstates given by

$$\psi_k(x) = \frac{1}{\sqrt{N_a}} \sum_{n=0}^{N_a-1} e^{iknd}\phi(x-na) \ , \tag{4.7}$$

where the wave vector k now labels the occupied electron states $\nu = k$. This solution is spin unpolarized and the local charge density associated with Eq. (4.7) is independent of the site index, $n_i^k = 1/N_a$. Correspondingly, the SIC correction to the electron potential, Eq. (3.14), only gives a uniform shift of the single-electron energies. The SIC correction to the total energy, Eq. (3.11), becomes

$$\Delta E^{\mathrm{SIC,PM}}/N_a = U\left[\frac{-1}{2N_a} + \frac{(a+b)}{N_a^{1/3}}\right] , \tag{4.8}$$

which tends to zero extremely slowly with the power $N_a^{-1/3}$ as $N_a \to \infty$ and is positive for all $N_a > 2$. We note that the total energy of the SIC-PM solution equals the LDA total energy plus the contribution given in Eq. (4.8). Thus, the LDA solution is simultaneously a paramagnetic solution of the SIC Hamiltonian only for truly infinite systems.

Both the SIC-AF and the LDA total energies converge very rapidly as a function of the system size. On physical grounds, one therefore expects the SIC-PM solution to approach the LDA solution also for reasonable system sizes. Actually, however, this is not the case due to the dependence of the SIC energy on the individual electron densities, as follows from Eq. (4.8). In Figs. 16(a) and 16(b), the total energies for the LDA, the localized antiferromagnetic SIC-AF, and the delocalized paramagnetic SIC-PM solutions of the SIC-LSD Hamiltonian are depicted as a function of the number of atoms $N_a = 2^n$ in the lattice. One can see that even for long chains with more than 2000 atoms *the relative ordering* of the SIC-PM versus SIC-AF total energy still differs from the ordering of the (paramagnetic) LDA versus SIC-AF energy.

These strong finite-size effects make it clear that the paramagnetic solution of the SIC-LSD Hamiltonian is unpractical to predict AF to PM transitions in solids.

C. Antiferromagnetic solutions — comparison of the SIC-LSD and LSD method

An alternative procedure to determine AF to PM transitions in extended systems is to compare the SIC-LSD with the LSD solutions. The LSD equations possess Bloch-type extended AF or PM solutions. For sufficiently large U, the LSD ground state is spin polarized whereas it converges towards the PM LDA solution for small U. For truly infinite systems, the LSD solution is also a solution of the SIC-LSD Hamiltonian since the SIC correction is zero for translational invariant one-electron states. Consequently, for infinite chains, the true ground state of the SIC-LSD Hamiltonian is the lower of the AF SIC-LSD solution and the LSD solution.

In Fig. 17 we show the results for the total energy per atom for an infinite linear Hubbard chain at half-filling as predicted by the LDA, the LSD, and the SIC-LSD method, and compare it to the exact ground-state energy

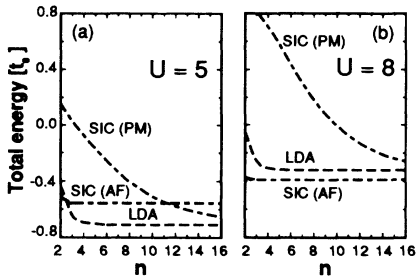

FIG. 16. Calculated total energy in the one-dimensional half-filled Hubbard model as a function of the lattice size 2^n for the antiferromagnetic (AF) and paramagnetic (PM) solutions of the SIC-LSD Hamiltonian for $U=5$ and 8. For comparison, the results of the LDA method are also depicted.

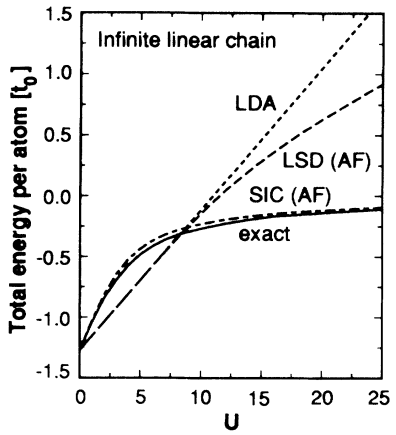

FIG. 17. Comparison of the calculated total energies in the one-dimensional half-filled Hubbard model for an infinite chain of atoms, calculated exactly by the SIC-LSD (AF-type solution), the LSD (AF-type solution), and the LDA (paramagnetic) method, respectively.

of the Hubbard Hamiltonian obtained by Lieb and Wu.[22] This figure suggests a phase transition from the extended LSD ground state to the AF SIC-LSD state for $U \approx 9$. In contrast, the exact total energy exhibits no transition and is much closer to the AF SIC-LSD energy than to the LSD energy *even for small values of U*. The same conclusion holds for the energy gap and the previously discussed correlation functions. For all of these properties, the AF SIC-LSD solutions are in excellent agreement with the exact solutions even though the former is higher in total energy than the LSD solution.

This forces one to conclude that the energy crossing between the paramagnetic LDA (or LSD) and the antiferromagnetic SIC-LSD solution for infinite systems has no physical significance, at least in the case of Hubbard-like models. Another conclusion is that the AF SIC state appears to be meaningful even in the regime of U values where the SIC correction to the total energy is positive.

One may ask why the SIC-LSD Hamiltonian yields localized Heitler-London-type AF solutions even for such small values of U. The reason lies in the one-electron SIC potential $V_i^{\mathrm{SIC},\nu}$, Eq. (3.14), which is always attractive on the site $x_i = x_\nu$ at which the electron ν is centered. Actually, the exchange-correlation functional parameters used in this work give $V_i^{\mathrm{SIC},\nu} < 0$ provided $n_{i\nu} > 0.47$. Any localized SIC solution is characterized by a local occupancy $n_{i\nu}$ which is larger than this value. In particular, already for $U = 0$, we find the squared amplitude of the Wannier state $w(x - x_\nu)$ for the valence band of the one-dimensional half-filled Hubbard model at $x = x_\nu$ to be 0.5. Whereas a local occupancy exceeding $n_{i\nu} = 0.47$ suffices to obtain an attractive on-site SIC potential, Eq. (3.11) shows that a much larger occupancy, namely $n_{i\nu} = 0.87$, is necessary to obtain a negative contribution to the total SIC energy. Such highly localized states form only for $U \geq 5$.

D. Charge-density-wave solutions

For the one-dimensional Hubbard chain at half-filling, we have also found commensurate charge-density-wave (CDW) solutions of the SIC Hamiltonian with a wavelength equal to twice the lattice constant. The CDW solution is paramagnetic and characterized by a modulation in the site occupancy. The one-electron states are localized. The total energy of this CDW solution lies in between the total energy of the localized and the delocalized SIC-LSD solutions.

E. Initial conditions and parametrizations

We have performed detailed checks to ensure that the results presented in this paper do not depend sensitively on the chosen parametrization of the exchange-correlation functional $E_{\mathrm{xc}}^{\mathrm{LSD}}$ in Eq. (3.9). There is no qualitative change in the results by changing the parameters a and b or the power dependence of $E_{\mathrm{xc}}^{\mathrm{LSD}}$ on the local density by as much as 50%. Also, we point out that it is not possible to obtain overall better agreement between LSD and exact results by altering one of these parameters. Let us consider, for example, the energy gap in the LSD method. For $U \to \infty$, one has $E_{\mathrm{gap}}^{\mathrm{LSD}} \sim \frac{8}{3} bU$, whereas the exact energy gap $E_{\mathrm{gap}}^{\mathrm{exact}} \sim U$. The requirement $E_{\mathrm{gap}}^{\mathrm{LSD}} = E_{\mathrm{gap}}^{\mathrm{exact}}$ would imply $b = \frac{3}{8} \approx a$, giving a functional $E_{\mathrm{xc}}^{\mathrm{LSD}}$ which leads to unphysical results.

F. Summary

Let us summarize the main results of this paper. We have studied in detail the self-interaction-corrected local-spin-density method (SIC-LSD) and applied it to a highly correlated many-electron system including phonons, namely the Hubbard-Peierls model. An efficient numerical algorithm was developed which allows one to find fully self-consistent solutions of the SIC-LSD equations. They are free of any symmetry constraints. Thus, this method yields spin-density-wave or charge-density-wave solutions for any band filling and for frozen phonon configurations where the symmetry of the one-electron states is not known *a priori*.

In the case of the 1D and 2D Hubbard-Peierls model, the antiferromagnetic solution of the SIC-LSD equations yields total energies, energy gaps, and charge/spin correlation functions which are generally in excellent agreement with the exact properties of the many-body Hamiltonian (which have been calculated for small system sizes). Only those electronic properties of low-dimensional systems which depend critically on spin quantum fluctuations are not accurately predicted by the SIC-LSD method. However, the method always provides a substantial improvement on the standard local-density theory in the whole range of the Hubbard repulsion parameter U. For infinite systems and small U, however, the antiferromagnetic solution of the SIC Hamiltonian, is not the global minimum of the total-energy functional. This may well be an artifact associated with the Hubbard model since realistic SIC calculations of transition-metal oxides predict the correct metallic or insulating ground state.[20]

Most importantly, the self-interaction-corrected local-spin-density method provides a physically correct description of localized states in solids or molecules interacting with extended states.

ACKNOWLEDGMENTS

This work was supported in part by the Deutsche Forschung Gemeinschaft under project SFB 348 and in the early stages by the Fonds zur Förderung der wissenschaftlichen Forschung in Österreich. Enumerous helpful and clarifying discussions with Axel Svane and Ole Gunnarsson are gratefully acknowledged.

APPENDIX: DETERMINATION OF LAGRANGE MULTIPLIERS

In this appendix we discuss our choice of the Lagrange multipliers in Eq. (2.23). We require $\tilde{E}_{\rm tot}$ to be stationary with respect to ψ_ν and with respect to ψ_ν^*. The projection of the corresponding derivatives of $\tilde{E}_{\rm tot}$ onto $|\psi_{\nu''}\rangle$ yields $2\times N\times N$ equations for the same number of unknown Lagrange multipliers:

$$0=\langle\psi_{\nu''}|H_\nu|\psi_\nu\rangle+\mu_{\nu\nu''}+\sum_{\nu'}\tilde{\mu}_{\nu\nu'}\langle\psi_{\nu''}|V_{\nu'}-V_\nu|\psi_{\nu'}\rangle\ , \tag{A1}$$

$$0=\langle\psi_{\nu''}|H_{\nu''}|\psi_\nu\rangle+\mu_{\nu\nu''}+\sum_{\nu'}\tilde{\mu}_{\nu'\nu''}\langle\psi_{\nu'}|V_{\nu'}-V_{\nu'}|\psi_\nu\rangle\ . \tag{A2}$$

For $\nu=\nu''$, these equations leave $\tilde{\mu}_{\nu\nu}$ undetermined but give

$$\mu_{\nu\nu}=-\langle\nu|H_\nu|\nu\rangle\ , \tag{A3}$$

where $|\nu\rangle\equiv|\psi_\nu\rangle$. Subtracting Eq. (A2) from Eq. (A1), one obtains a linear system of equations for $\tilde{\mu}_{\nu\nu'}$. This system has the trivial solution $\tilde{\mu}_{\nu\nu'}=0$. Noticeably, this is the only solution in general, as one can show by induction. The $N=2$ case reads, for example,

$$(\langle 2|V_2-V_1|2\rangle-\langle 1|V_2-V_1|1\rangle)\tilde{\mu}_{12}=0\ . \tag{A4}$$

Since $(\langle 2|V_2-V_1|2\rangle-\langle 1|V_2-V_1|1\rangle)$ is nonzero, $\tilde{\mu}_{12}$ must be equal to zero. Generally, the Lagrange multipliers at the extremum are given by

$$\mu_{\nu\nu'}=-\lambda_{\nu\nu'},\quad \tilde{\mu}_{\nu\nu'}=0,\quad \nu\nu'=1,\ldots,N\ . \tag{A5}$$

The Lagrange multipliers at the extremum are not necessarily the optimum choice far away from this limit, however. In particular, a preferable choice is given by the following expression:

$$\begin{aligned}\mu_{\nu\nu'}&=-\tfrac{1}{2}\{\lambda^*_{\nu'\nu}+\lambda_{\nu\nu'}\}\\&=-\tfrac{1}{2}\{\langle\nu'|H_\nu|\nu\rangle^*+\langle\nu|H_{\nu'}|\nu'\rangle\}\ ,\end{aligned} \tag{A6}$$

since it guarantees that the matrix λ is automatically Hermitian at the extremum. This can be shown by setting the gradient of the total energy, Eq. (2.22) with $\tilde{\mu}=0$, equal to zero, i.e.,

$$\frac{\delta\tilde{E}_{\rm tot}}{\delta\psi_\nu}=H_\nu|\nu\rangle+\sum_{\nu'}\mu_{\nu\nu'}|\nu'\rangle=0\ . \tag{A7}$$

Indeed, multiplying this equation by $\langle\nu''|$ and using the orthonormality of the orbital set $\{|\nu\rangle\}$, one obtains the Hermiticity of the matrix λ, provided Eq. (A6) is used for μ. In addition to the choice of Eq. (A6), the convergence can be considerably accelerated by including the Lagrange parameter $\tilde{\mu}_{\nu\nu'}$ in the form

$$\tilde{\mu}_{\nu\nu'}=\lambda^*_{\nu'\nu}-\lambda_{\nu\nu'}\ . \tag{A8}$$

This adds a term to the total-energy functional $\tilde{E}_{\rm tot}$ which is quadratic in the matrix λ and thus steepens the iteratively computed gradients.

[1]P. Hohenberg and W. Kohn, Phys. Rev. **136**, B864 (1964); W. Kohn and L. J. Sham, *ibid.* **140**, A1133 (1965).
[2]R. O. Jones and O. Gunnarsson, Rev. Mod. Phys. **61**, 689 (1989), and references therein.
[3]K. C. Hass, in *Solid State Physics*, edited by H. Ehrenreich, D. Turnbull, and P. Grosse (Academic, New York, 1989), Vol. 42, p. 213.
[4]J. P. Perdew and A. Zunger, Phys. Rev. B **23**, 5048 (1981).
[5]J. P. Perdew, Chem. Phys. Lett. **64**, 128 (1979); J. G. Harrison, J. Chem. Phys. **79**, 2265 (1983); J. G. Harrison, *ibid.* **78**, 4562 (1983); M. R. Pederson and Chun C. Lin, *ibid.* **88**, 1807 (1988); J. G. Harrison, Chem. Phys. Lett. **96**, 181 (1983); R. A. Heaton, M. R. Pederson, and Chun C. Lin, J. Chem. Phys. **86**, 258 (1987); P. Cortona, Phys. Rev. B **38**, 3850 (1988); Y. Guo and M. A. Whitehead, *ibid.* **40**, 28 (1989); K. A. Jackson and Chun C. Lin, *ibid.* **39**, 1557 (1989).
[6]M. R. Pederson, R. A. Heaton, and Chun C. Lin, J. Chem. Phys. **80**, 1972 (1984).
[7]M. R. Pederson, R. A. Heaton, and Chun C. Lin, J. Chem. Phys. **82**, 2688 (1985).
[8]R. A. Heaton, J. G. Harrison, and Chun C. Lin, Phys. Rev. B **28**, 5992 (1983).
[9]R. A. Heaton and Chun C. Lin, J. Phys. C **17**, 1853 (1984).
[10]S. C. Erwin and Chun C. Lin, J. Phys. C **21**, 4285 (1988).
[11]Yan Li, J. B. Krieger, M. R. Norman, and G. J. Iafrate, Phys. Rev. B **44**, 10437 (1991).
[12]N. Hamada and S. Ohnishi, Phys. Rev. B **34**, 9042 (1986); Y. Hatsugai and T. Fujiwara, *ibid.* **37**, 1280 (1988).
[13]Z. Szotek, W. M. Temmerman, and H. Winter, Physica B **172**, 19 (1991).
[14]R. A. Heaton, J. G. Harrison, and Chun C. Lin, Phys. Rev. B **31**, 1077 (1985); M. R. Pederson and B. M. Klein, *ibid.* **37**, 10319 (1988); K A. Jackson and Chun C. Lin, *ibid.* **38**, 12171 (1988); K. A. Jackson and Chun C. Lin, *ibid.* **38**, 947 (1990).
[15]J. G. Harrison, Phys. Rev. B **35**, 987 (1987); M. R. Pederson, R. A. Heaton, and J. G. Harrison, *ibid.* **39**, 1581 (1989).
[16]A. Svane and O. Gunnarsson, Phys. Rev. B **37**, 9919 (1988).
[17]A. Svane and O. Gunnarsson, Europhys. Lett. **7**, 171 (1988).
[18]Y. Ishii and K. Terakura, Phys. Rev. B **42**, 10924 (1990).
[19]J. A. Majewski, P. Vogl, and A. Svane, in *Electronic Properties of High-T_c Superconductors and Related Compounds*, edited by H. Kuzmany, M. Mehring, and J. Fink (Springer, Berlin, 1990), p. 397; this paper contains preliminary results of the model presented here.
[20]A. Svane and O. Gunnarsson, Phys. Rev. Lett. **65**, 1148 (1990).
[21]J. Hubbard, Proc. R. Soc. (London), Ser. A **276**, 238 (1963).

[22]E. H. Lieb and F. Y. Wu, Phys. Rev. Lett. **20**, 1445 (1968).
[23]H. Shiba, Phys. Rev. B **6**, 930 (1972).
[24]R. E. Peierls, *Quantum Theory of Solids* (Clarendon, Oxford, 1955), Chap. 5.
[25]For a review see, for example, V. J. Emery, IBM J. Res. Develop. **33**, 246 (1989); R. J. Birgeneau, Am. J. Phys. **58**, 28 (1990).
[26]G. Dopf, A. Muramatsu, and W. Hanke, Phys. Rev. Lett. **68**, 353 (1992).
[27]R. Car and M. Parrinello, Phys. Rev. Lett. **55**, 2471 (1985).
[28]I. Štich, R. Car, M. Parrinello, and S. Baroni, Phys. Rev. B **39**, 4997 (1989).
[29]M. P. Teter, M. C. Payne, and D. C. Allan, Phys. Rev. B **40**, 12 255 (1989).
[30]S. Kirkpatrick, C. D. Gellatt, Jr., and M. P. Vecchi, Science **220**, 671 (1983).
[31]T. M. Rice, Z. Phys. B **67**, 141 (1987).
[32]R. A. Harris and L. M. Falicov, J. Chem. Phys. **51**, 5034 (1969).
[33]P. Horsch, Phys. Rev. B **24**, 7351 (1981).
[34]D. Baeriswyl and K. Maki, Phys. Rev. B **31**, 6633 (1985).
[35]J. E. Hirsch, Phys. Rev. Lett. **51**, 296 (1983).
[36]S. Mazumdar and S. N. Dixit, Phys. Rev. Lett. **51**, 292 (1983); S. N. Dixit and S. Mazumdar, Phys. Rev. B **29**, 1824 (1984).
[37]D. Penn, Phys. Rev. B **142**, 350 (1966).
[38]J. A. Verges, E. Louis, P. S. Lomdahl, F. Guinea, and A. R. Bishop, Phys. Rev. B **43**, 6099 (1991).
[39]G. Kotliar and A. E. Ruckenstein, Phys. Rev. Lett. **57**, 1362 (1986).
[40]L. Lilly, A. Muramatsu, and W. Hanke, Phys. Rev. Lett. **65**, 1379 (1990).
[41]J. Hubbard, Proc. R. Soc. (London), Ser. A **281**, 401 (1964).
[42]M. Cyrot, J. Phys. (Paris) **33**, 125 (1972).
[43]M. C. Gutzwiller, Phys. Rev. **137**, A1726 (1965).
[44]P. G. McQueen and C. S. Wang, Phys. Rev. B **39**, 12 414 (1989).
[45]S. N. Coppersmith and Clare C. Yu, Phys. Rev. B **39**, 11 464 (1989).
[46]H. Q. Lin, J. E. Hirsch, and D. J. Scalapino, Phys. Rev. B **37**, 7359 (1988).
[47]J. Callaway, D. P. Chen, and R. Tang, Phys. Rev. B **35**, 3705 (1987).
[48]A. Parola, S. Sorella, S. Baroni, M. Parrinello, and E. Tosatti, Int. J. Mod. Phys. B **3**, 1865 (1989).
[49]A. Parola, S. Sorella, M. Parrinello, and E. Tosatti, Phys. Rev. B **43**, 6190 (1991).
[50]J. E. Hirsch, Phys. Rev. B **31**, 4403 (1985).
[51]J. E. Hirsch, Phys. Rev. Lett. **62**, 591 (1989).
[52]S. R. White, D. J. Scalapino, R. L. Sugar, E. Y. Loh, J. E. Gubernatis, and R. T. Scalettar, Phys. Rev. B **40**, 506 (1989).
[53]Y. Zhang and J. Callaway, Phys. Rev. B **39**, 9397 (1989).
[54]S. Sorella, S. Baroni, R. Car, and M. Parrinello, Europhys. Lett. **8**, 663 (1989).
[55]S. Sorella, A. Parola, M. Parrinello, and E. Tosatti, Int. J. Mod. Phys. B **3**, 1875 (1989).
[56]A. Moreo, D. J. Scalapino, R. L. Sugar, S. R. White, and N. E. Bickers, Phys. Rev. B **41**, 2313 (1990).
[57]S. Tang and J. E. Hirsch, Phys. Rev. B **37**, 9546 (1988).
[58]S. Tang and J. E. Hirsch, Phys. Rev. B **39**, 12 327 (1989).
[59]S. Mazumdar, Phys. Rev. B **39**, 12 324 (1989).
[60]F. C. Zhang and P. Prelovsek, Phys. Rev. B **37**, 1569 (1988).
[61]O. Gunnarsson and K. Schönhammer, Phys. Rev. Lett. **56**, 1968 (1986).
[62]N. D. Mermin and H. Wagner, Phys. Rev. Lett. **17**, 1133 (1966).
[63]R. Natarajan and D. Vanderbilt, J. Comp. Phys. **82**, 218 (1989).
[64]E. H. Lieb, Phys. Rev. Lett. **62**, 1201 (1989).
[65]J. P. Perdew and M. Levy, Phys. Rev. Lett. **51**, 1884 (1983); L. J. Sham and M. Schlüter, Phys. Rev. B **32**, 3883 (1985).
[66]W. Metzner and D. Vollhardt, Phys. Rev. B **37**, 7382 (1988).
[67]E. Fradkin, *Field Theories of Condensed Matter Systems* (Addison-Wesley, Redwood City, 1991), p. 23.
[68]E. Dagotto, A. Moreo, R. L. Sugar, and D. Toussaint, Phys. Rev. B **41**, 811 (1990).
[69]H. J. Schullz, Phys. Rev. Lett. **64**, 1445 (1990).
[70]W. P. Su, J. R. Schriefer, and A. J. Heeger, Phys. Rev. Lett. **42**, 1698 (1979).